Supplementary Information for 'Membrane/Toxin Interaction Energetics via Serial Multi-Scale Molecular Dynamics Simulations'

Chze Ling Wee, Martin Ulmschneider, and Mark S.P. Sansom

Toxin Structures in the AT Simulations

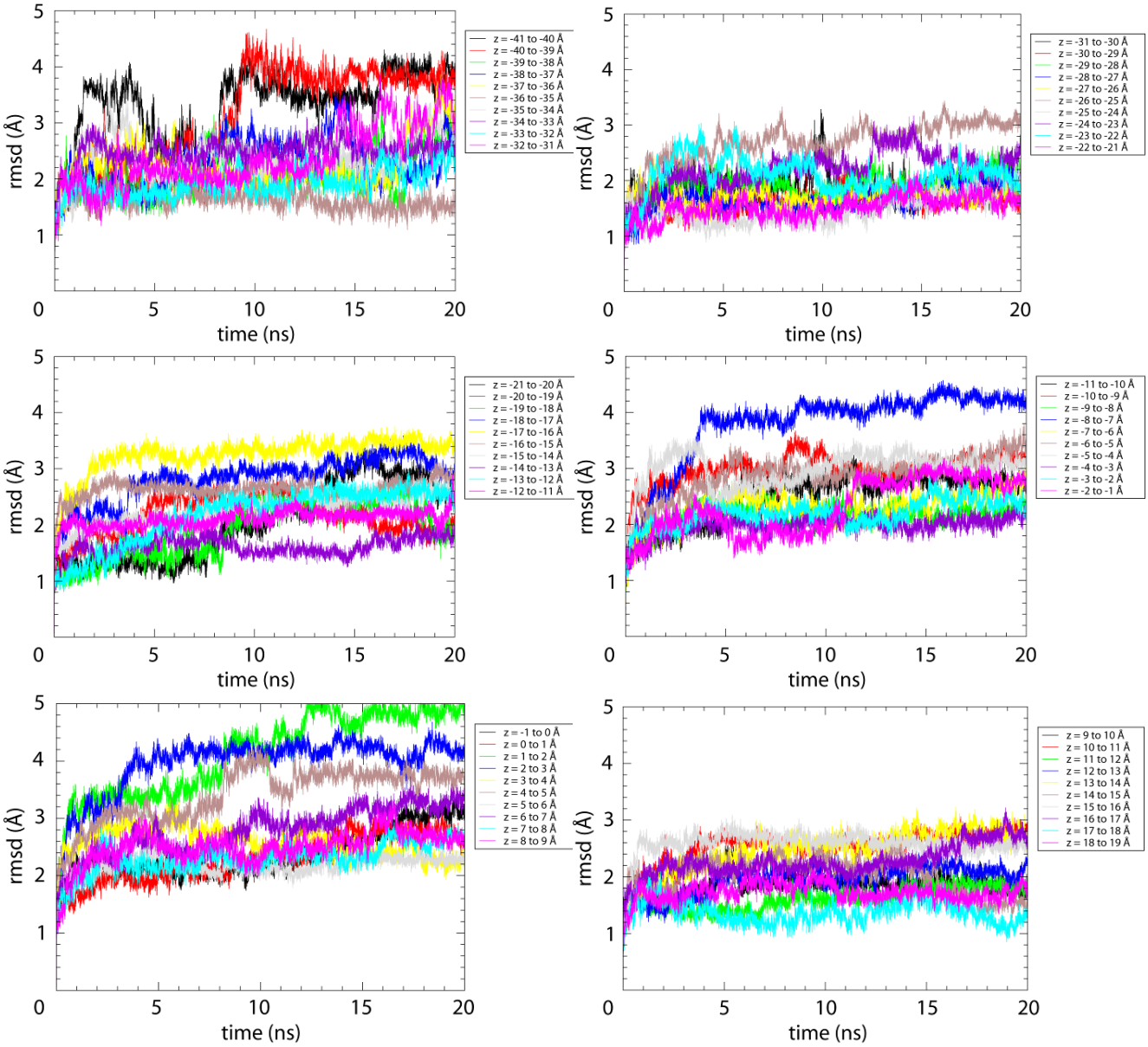

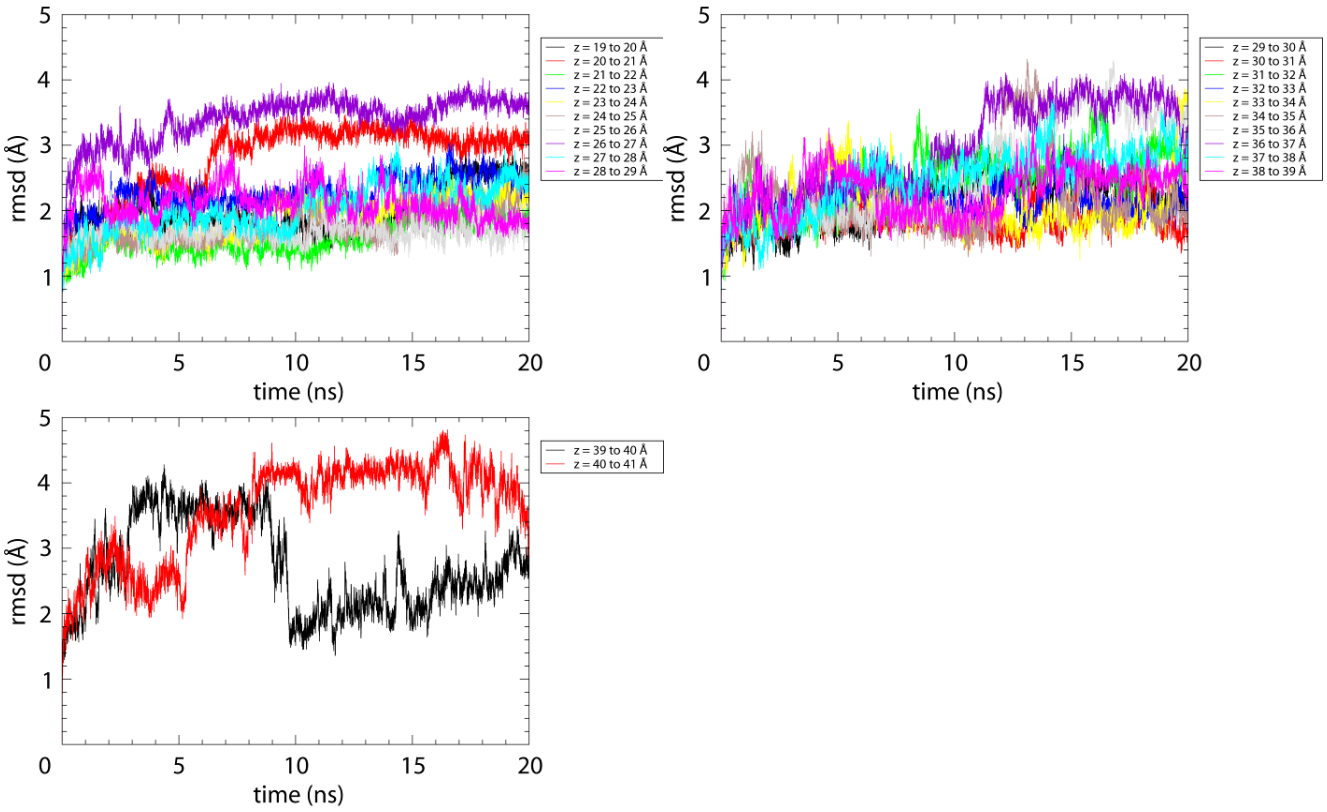

Figure S1: Root-mean-squared-deviation of the C_α atoms of VSTx1 (after a C_α least-squared-fit to the initial toxin structure).

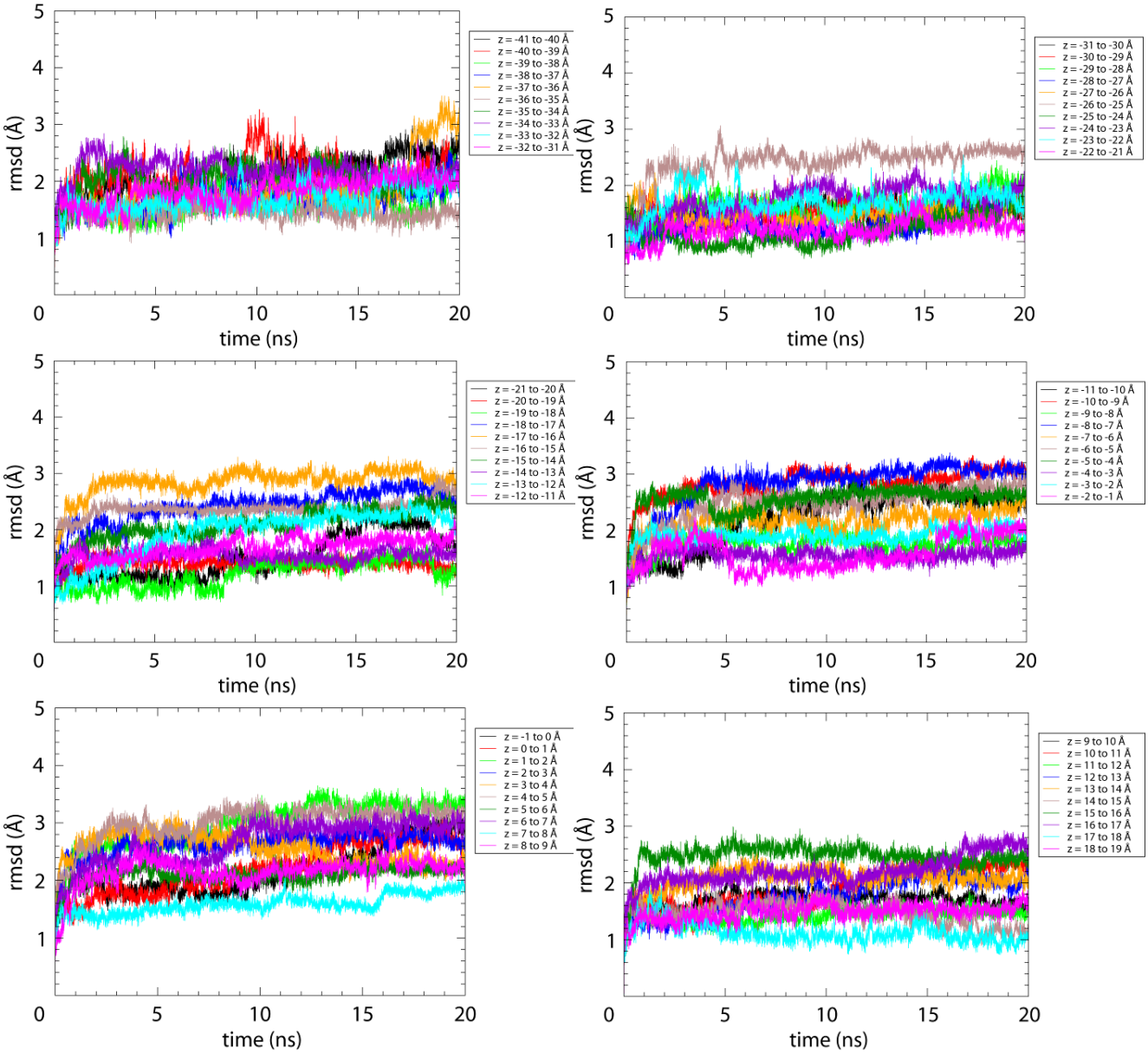
rmsd (Å)
time (ns)
z = -41 to -40 Å
z = -40 to -39 Å
z = -39 to -38 Å
z = -38 to -37 Å
z = -37 to -36 Å
z = -36 to -35 Å
z = -35 to -34 Å
z = -34 to -33 Å
z = -33 to -32 Å
z = -32 to -31 Å
z = -31 to -30 Å
z = -30 to -29 Å
z = -29 to -28 Å
z = -28 to -27 Å
z = -27 to -26 Å
z = -26 to -25 Å
z = -25 to -24 Å
z = -24 to -23 Å
z = -23 to -22 Å
z = -22 to -21 Å
z = -21 to -20 Å
z = -20 to -19 Å
z = -19 to -18 Å
z = -18 to -17 Å
z = -17 to -16 Å
z = -16 to -15 Å
z = -15 to -14 Å
z = -14 to -13 Å
z = -13 to -12 Å
z = -12 to -11 Å
z = -11 to -10 Å
z = -10 to -9 Å
z = -9 to -8 Å
z = -8 to -7 Å
z = -7 to -6 Å
z = -6 to -5 Å
z = -5 to -4 Å
z = -4 to -3 Å
z = -3 to -2 Å
z = -2 to -1 Å
z = -1 to 0 Å
z = 0 to 1 Å
z = 1 to 2 Å
z = 2 to 3 Å
z = 3 to 4 Å
z = 4 to 5 Å
z = 5 to 6 Å
z = 6 to 7 Å
z = 7 to 8 Å
z = 8 to 9 Å
z = 9 to 10 Å
z = 10 to 11 Å
z = 11 to 12 Å
z = 12 to 13 Å
z = 13 to 14 Å
z = 14 to 15 Å
z = 15 to 16 Å
z = 16 to 17 Å
z = 17 to 18 Å
z = 18 to 19 Å

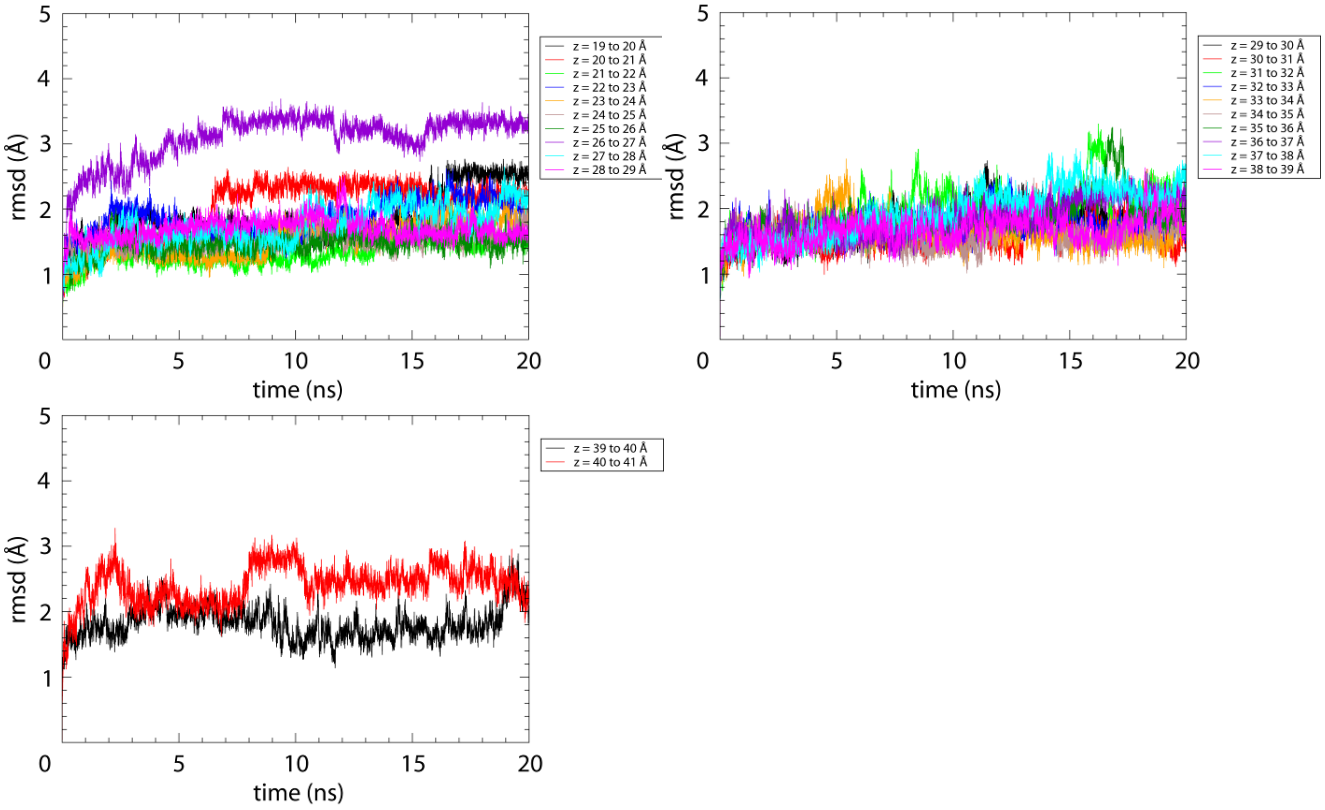

Figure S2: Root-mean-squared-deviation of the C_α atoms of VSTx1 (after a C_α least-squared-fit to the initial toxin structure) ignoring the C_α atoms of the N-terminal residue and the C-terminal two residues.

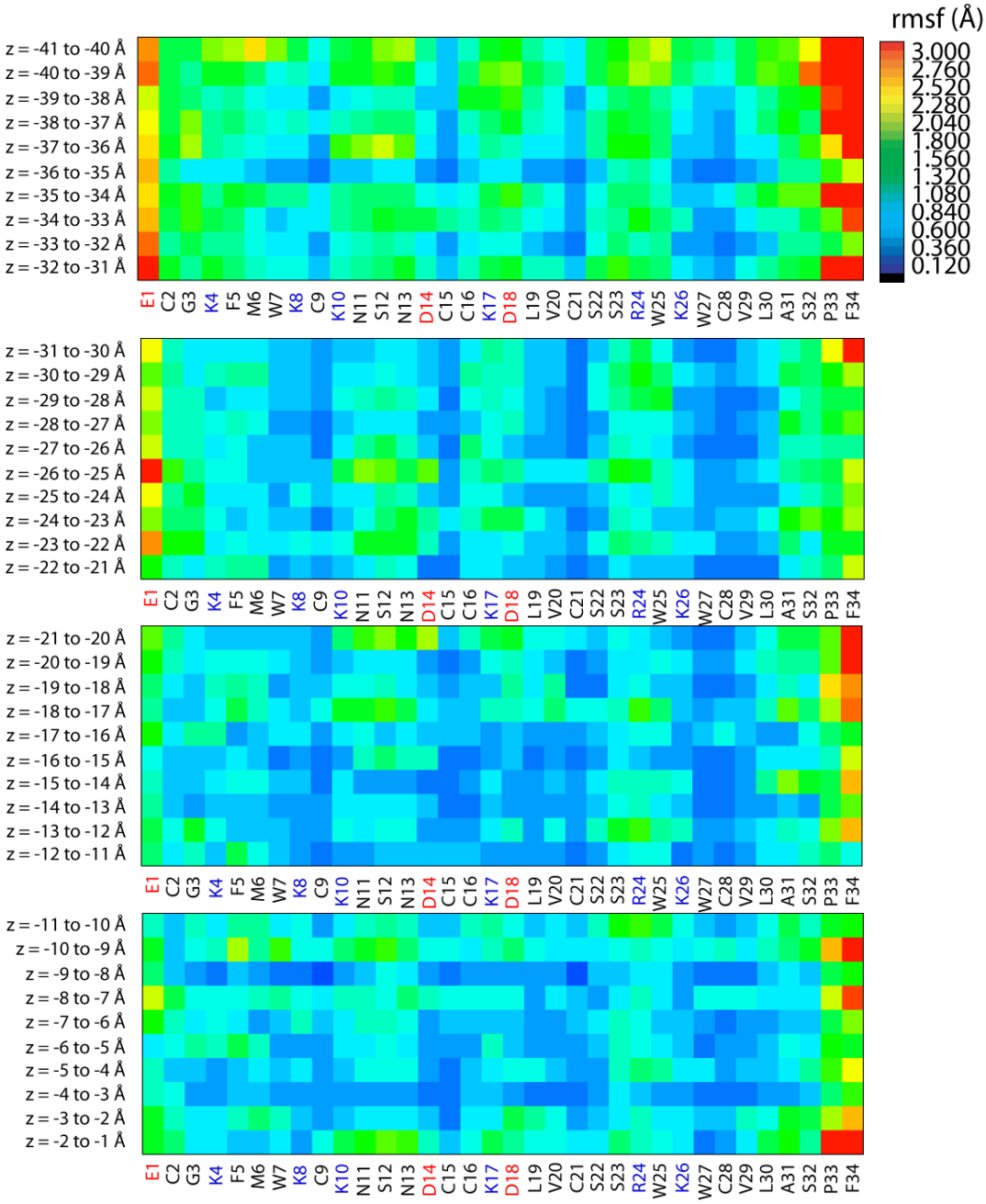

Figure S3: Root-mean-squared-fluctuation of the C_α atoms of VSTx1 in windows z = -41 to -1 Å (time-averaged over 20 ns and after a C_α least-squared-fit to the initial toxin structure). Basic and acidic residues are labeled blue and red respectively. All other residues are labelled black.

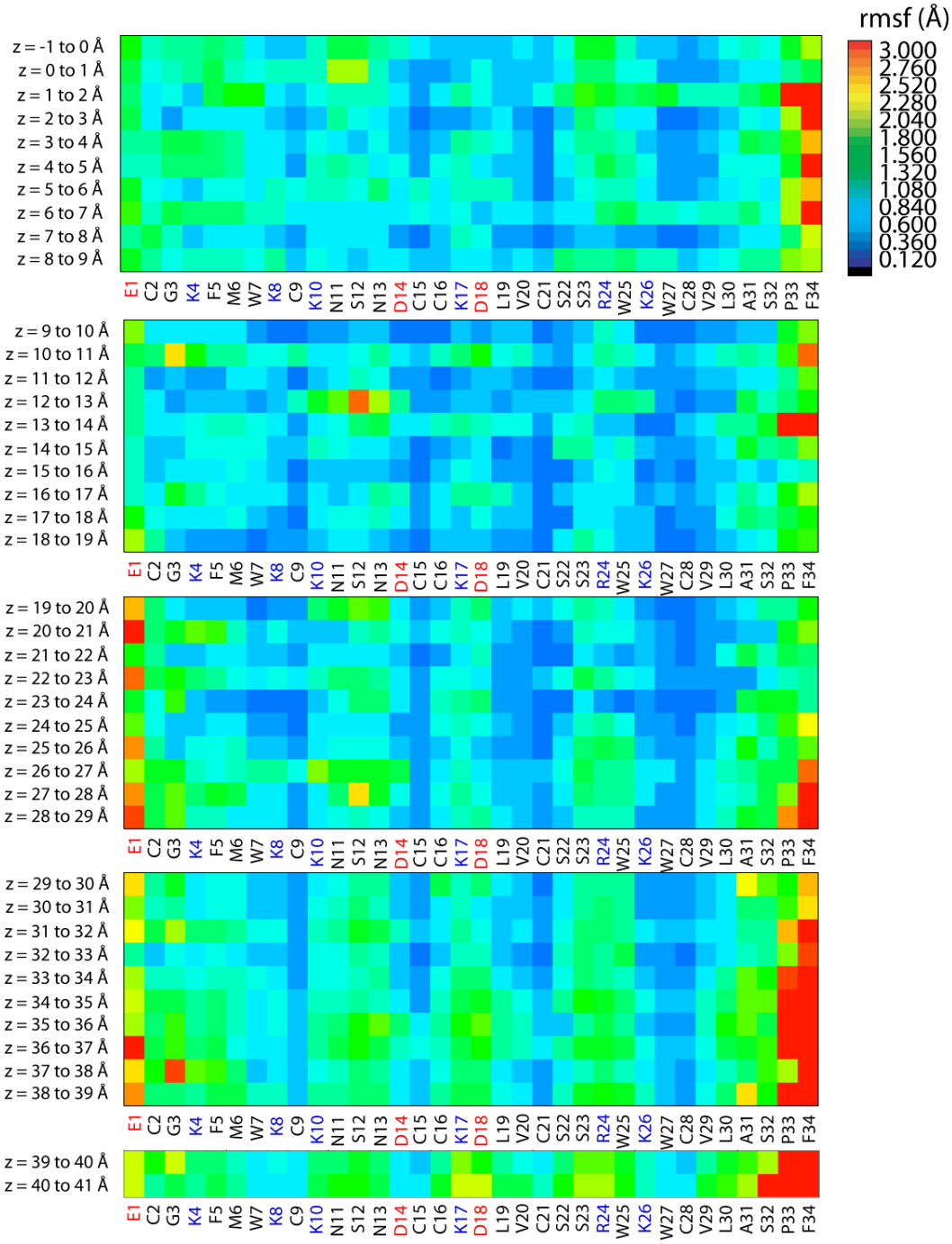

Figure S4: Root-mean-squared-fluctuation of the C_α atoms of VSTx1 in windows z = -1 to 41 Å (time-averaged over 20 ns and after a C_α least-squared-fit to the initial toxin structure). Basic and acidic residues are labeled blue and red respectively. All other residues are labelled black.

Convergence in the AT Free Energy Profiles

We investigated convergence in the AT PMF profile by splitting the distributions from 17 to 20 ns/window into non-overlapping blocks to compute the mean ± 1 SD at each *z*. The AT profile had sufficiently converged.

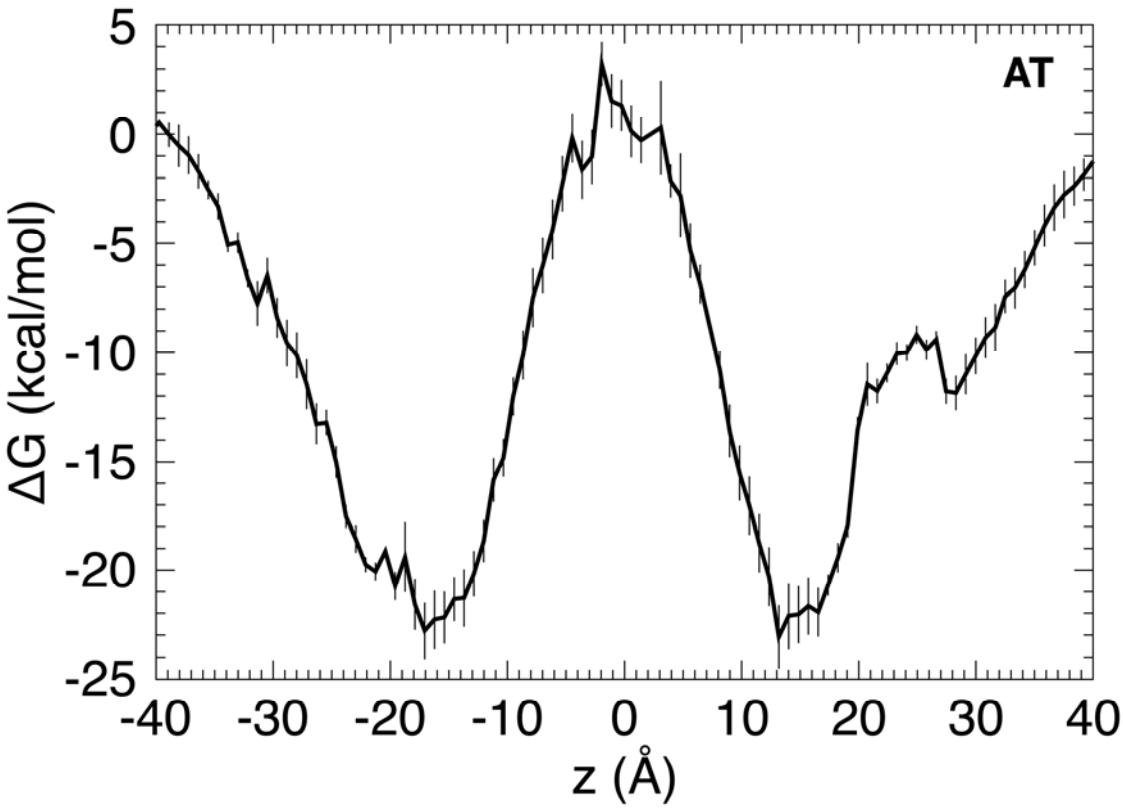

Figure S5: Block analyses suggest the AT PMF profile had sufficiently converged. Mean ± 1 SD.

Asymmetry in the Bilayer in the AT Simulations

We counted the number of lipids in the extracellular (EC) and intracellular (IC) leaflets of the POPC bilayer in the AT simulations (Fig. S6). Starting with a pre-equilibrated POPC bilayer consisting of 128 lipids with 64 lipids per leaflet (courtesy of Peter Tieleman; moose.bio.ucalgary.ca), we modelled VSTx1 in the bilayer and a few lipids had to be removed to accommodate the toxin (see main text for details). In all AT windows, no more than 7 lipids were removed. However, the number of lipids removed from EC and IC leaflets was not identical (i.e. no symmetry about $z = 0$ Å). This may explain the asymmetry in the AT PMF profile about $z = 0$ Å.

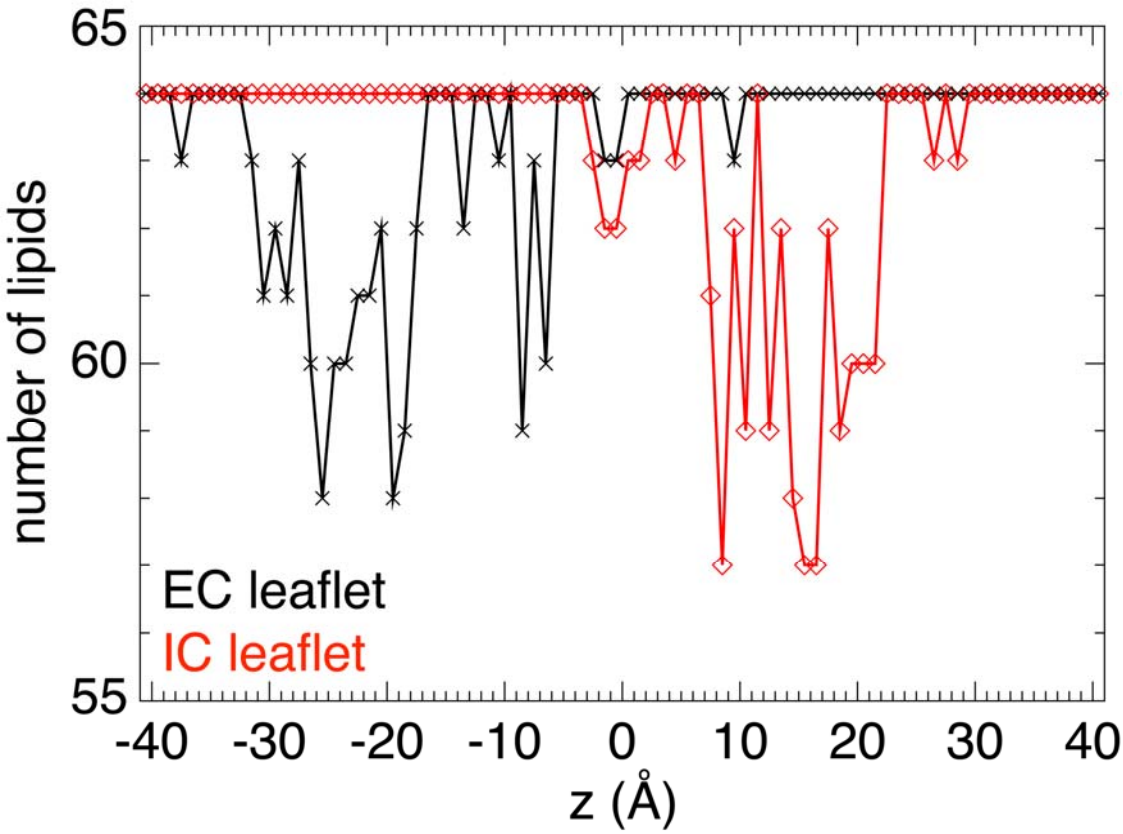

Figure S6: Number of lipids in the EC and IC leaflets of the POPC bilayer in the AT windows.

Lipid Structure near the Toxin

In Fig. S7, we calculated the average order parameters (*Scd*; averaged over 17 to 20 ns/window) of the palmitoyl chain of the POPC lipids in the intracellular (IC) leaflet when the toxin was located between *z* = 15 to 41 Å (i.e. VSTx1 spanning the width of the IC leaflet to VSTx1 in bulk water). For C2 to C9 of the palmitoyl chains (Fig. S7A), *Scd* ~ 0.18 to 0.25. There was no clear trend over *z*. For C10 to C15 (Fig. S7B), *Scd* ~ 0.10 and 0.20, reflecting increased disorder further along the palmitoyl chains. Unlike the *Scd* values of C2 to C9, there was a modest but systematic decrease in the *Scd* values of C10 to C15 from *z* = 41 to 15 Å. Thus, the ends of the lipid tails became more disordered to accommodate VSTx1.

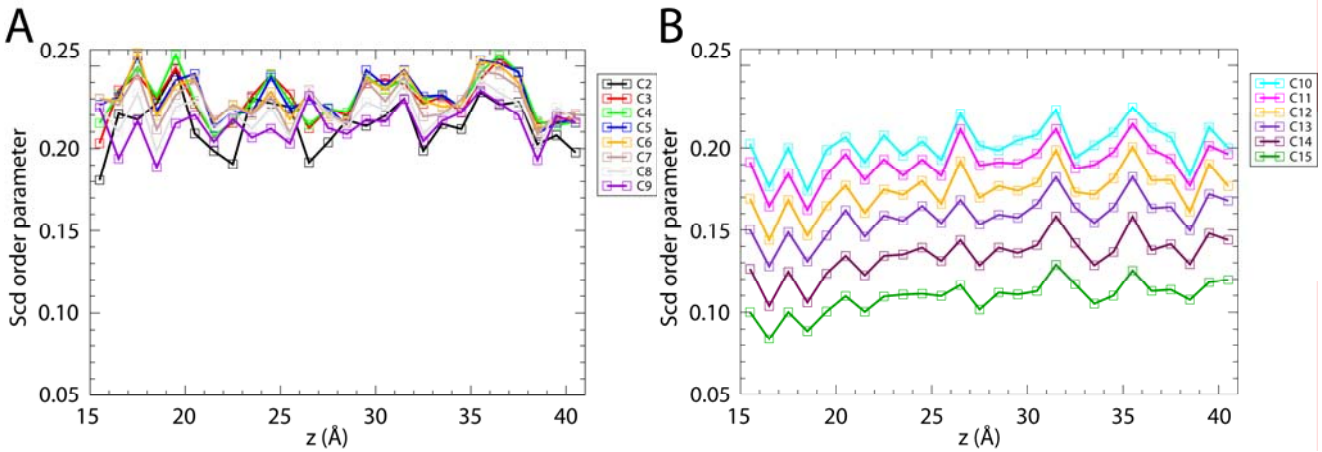

Figure S7: Average order parameters (*Scd*) of the palmitoyl chain of POPC lipids in the intracellular (IC) leaflet for windows *z* = 15 to 41 Å. This corresponds to toxin locations where VSTx1 spanned the width of the IC leaflet to toxin locations in bulk water (see Fig. 2 in main text for reference). Averages were taken over 17 to 20 ns/window. (A) *Scd* for C2 to C9. (B) *Scd* for C10 to C15.

Fig. S8 shows the conformations of several lipids near VSTx1 when the toxin was located close to the free energy well (i.e. at its optimal location of interaction with the POPC bilayer; window *z* = -17 to -16 Å). The acyl chains 'wrapped' over the hydrophobic face of the toxin. Interestingly, recent experimental studies suggest that binding of VSTx1 to model bilayers triggers modest alteration in membrane structure and dynamics [1].

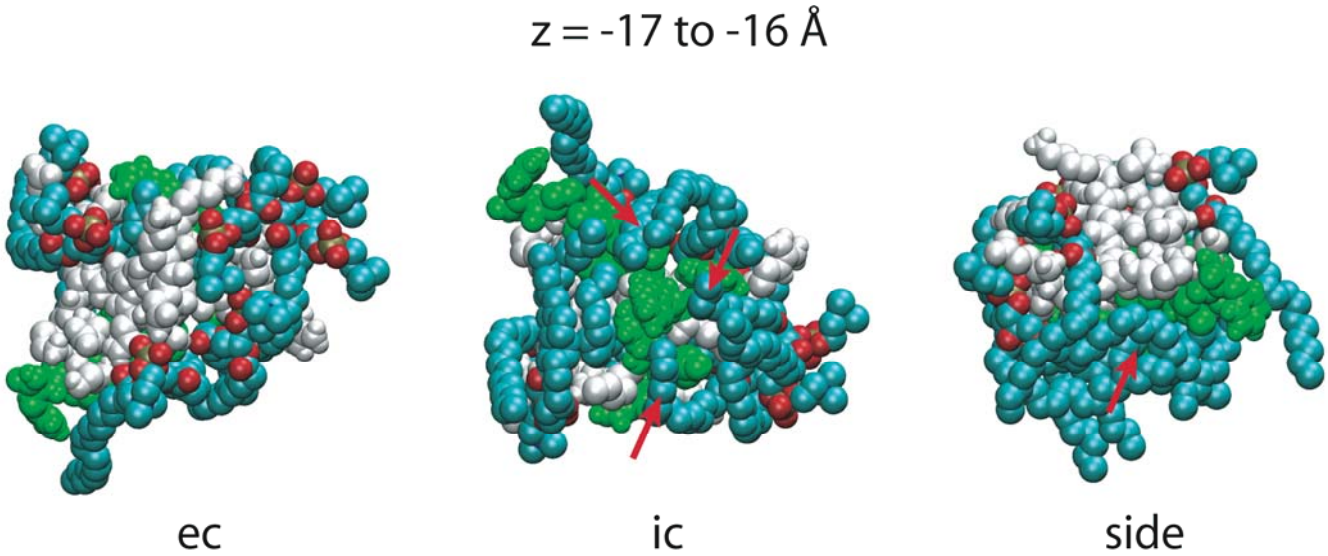

Figure S8: Conformations of lipids near VSTx1. Snapshots were from window *z* = -17 to -16 Å (i.e. when the toxin was located close to the free energy well). Extracellular (EC), IC and side views of the toxin and the surrounding lipids are shown. Hydrophobic residues of the toxin are coloured green. Polar and charged residues of the toxin are coloured white. POPC carbon, oxygen, nitrogen and phosphorus atoms are coloured cyan, red, blue and gold respectively. For clarity, all other lipids, waters and counterions are not shown. Red arrows highlight the 'wrapping' of lipid acyl chains over the hydrophobic face of the toxin.

Justification of a Multi-Scale Approach for Computing Free Energies

We performed 3 additional simulations, each of duration 45 ns (different initial velocities; *test sim 1 - 3*), with VSTx1 located close to the interfacial free energy well but with a non-optimal initial orientation (i.e. 'upside-down' relative to the bilayer). Starting with window z = -18 to -17 Å at 0 ns, we rotated the toxin 180 º about the x-axis such that the polar residues of VSTx1 were directed at the lipid tails and the hydrophobic residues, exposed to the lipid headgroups (Fig. S9A). A biasing umbrella potential was present, as in window z = -18 to -17 Å.

In Fig. S9B, we plot the time evolution of θ of *test sim 1 – 3*, compared against window z = -18 to -17 Å. In window z = -18 to -17 Å, θ equilibrated by 5 ns to 5.3 ± 2.1 º (average ± 1 SD; averaged over 5 to 20 ns). In *test sim 1 - 3*, a slow drift in θ was observed without apparent equilibration over 45 ns. In *test sim 1*, θ drifted from ~ 155 º to ~ 130 º over 45 ns (i.e. a change of only ~ 25 º). The smoother energy landscape of a CG potential, in contrast, allows θ to change by up to ~ 125 º over 10 ns (on a CG timescale) [2]. It is clear we would need to simulate well in excess of 45 ns for toxin orientation to relax in the AT simulations.

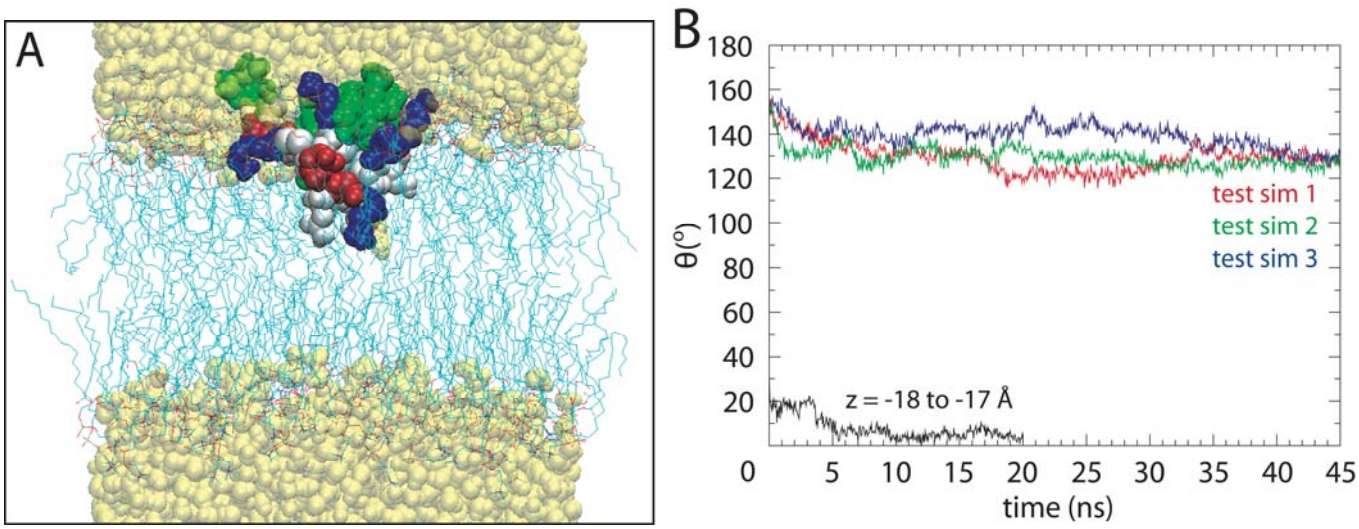

Figure S9: Simulations with a non-ideal initial orientation of VSTx1 in the bilayer (*test sim 1 - 3*; different initial velocities). (A) Starting with window z = -18 to -17 Å at 0 ns, we rotated the toxin 180 º about the x-axis such that the polar residues of VSTx1 were directed at the lipid tails and the hydrophobic residues, exposed to the lipid headgroups. Snapshot at 0 ns. The basic, acidic, polar and hydrophobic residues of VSTx1 are coloured blue, red, white and green respectively. POPC carbon, oxygen, nitrogen and phosphorus atoms are coloured cyan, red, blue and gold respectively in a lines representation. Waters are coloured yellow. Counterions are not shown. (B) Time evolution of the angle of the hydrophobic moment of VSTx1 relative to the bilayer normal (θ) for *test sim 1 - 3*. θ of window z = -18 to -17 Å is shown for comparison.

References

1. Krepkiy, D.; Mihailescu, E.; Gawrisch, K.; Swartz, K. J., Influence of a potassium channel voltage sensor toxin on the structure of lipid membranes. *Biophys. J.* **2007,** 2007 Biophysical Society Meeting Abstracts, Supplement, 295a.
2. Wee, C. L.; Gavaghan, D.; Sansom, M. S. P., Lipid bilayer deformation and free energy of interaction of a Kv channel gating modifier toxin. *Biophys. J.* **2008,** 95, 3816-3826.